

HARLAN L. MCKIM  
CAROLYN J. MERRY  
U.S. Army Cold Regions Research and Engineering Laboratory  
Hanover, NH 03755  
ROBERT W. LAYMAN  
Department of Physics and Astronomy  
Dartmouth College  
Hanover, NH 03755

# Water Quality Monitoring Using an Airborne Spectroradiometer

A 500-channel airborne spectroradiometer was tested under laboratory and field conditions for Corps of Engineers use.

## INTRODUCTION

THE U.S. ARMY CORPS OF ENGINEERS is responsible for the maintenance of all navigable waterways, many shorelines, and the Corps flood control reservoirs in the United States. A knowledge of the amount and changes in the level of suspended organic and inorganic sediment is an important factor in the management of these resources. There are certain areas where monitoring low turbidity is important, such as public water supply intakes and

particularly suited to the requirements of the Corps for reasons stated below, and consequently was used for this study. The purpose of this study was to evaluate the usefulness of the Chiu-Collins spectroradiometer to serve the needs of the Corps of Engineers.

## THE CHIU-COLLINS SPECTRORADIOMETER

The heart of the Chiu-Collins spectroradiometer system is a Princeton Applied Research Optical

---

**ABSTRACT:** *An airborne 500-channel spectroradiometer developed and built by Chiu and Collins (1978) was tested to determine its usefulness to the U.S. Army Corps of Engineers for monitoring the suspended load in lakes, reservoirs, and waterways. Field and laboratory experiments were run to test and evaluate the radiometer's response to various levels of suspended organic and inorganic materials. A procedure to separate the sun glint, which is often a large percentage of the recorded signal, from the total signal was investigated. Results indicated that the accuracy of the airborne water turbidity measurements was sufficient to meet certain monitoring requirements of the Corps of Engineers.*

---

ecologically sensitive areas like coral reefs. Also important is the monitoring of dispersion of turbidity around a dredge. An airborne system to monitor water turbidity, both qualitatively and quantitatively, would provide an effective means of determining water quality quickly and economically.

There have been a number of investigators who have studied the effect of subsurface scattering on the spectral distribution of reflected global radiance with a variety of spectroradiometers (Hodgson *et al.*, 1981; Richie *et al.*, 1976; Moore 1980). However, the instrument of Chiu and Collins (1978) is

Multichannel Analyzer (OMA) (Figure 1). The OMA detector is an array of light-sensitive silicon diodes on 8- $\mu\text{m}$  centers located on the inner face of a vidicon tube. The diodes are read by an electron beam 20  $\mu\text{m}$  in diameter. The beam scans the diode array with a raster of 500 lines, each line being one "monochromatic" channel of a complete spectrum. The output of a 0.33-metre Ebert spectrograph is focused on the diode array in such a way that the image of the entrance slit of the spectrograph is parallel to the lines of the raster. The diode array is scanned at the rate of 64 microseconds per line

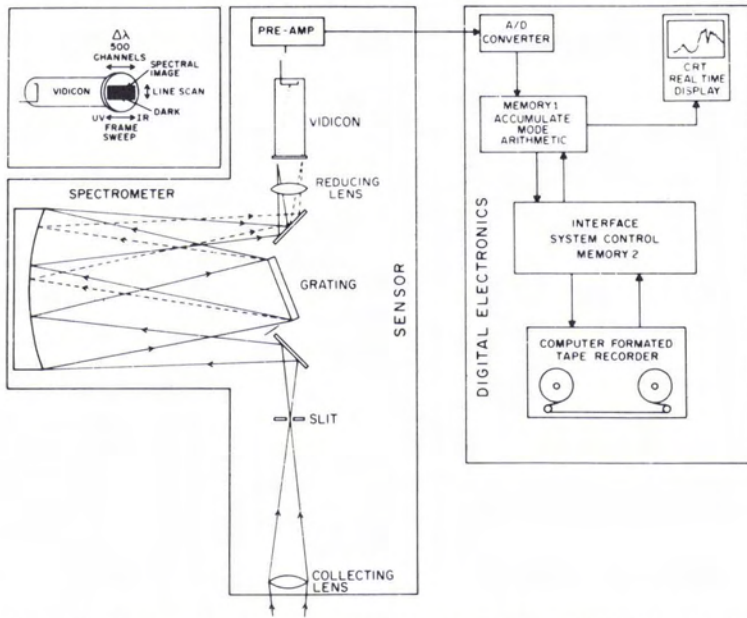


FIG. 1. Schematic diagram of airborne spectroradiometer system (after Chiu and Collins, 1978).

(channel) or 32 milliseconds for a complete frame of 500 lines. The output of the vidicon is stored in a 500-channel memory. A complete spectrum is defined as the sum of one or more frames. When the desired number of frames is accumulated, the data in memory are transferred to magnetic tape and the memory cleared for the next spectrum. In this study a spectrum consisted of ten frames; therefore, a complete spectrum was recorded every 320 milliseconds.

The 0.33-metre Jarrell Ash spectrometer has a spectral range of 400 to 1100 nm. The dispersion is 700 nm over 500 channels or 1.4 nm per channel. At 486.13 nm and 656.28 nm the measured resolution is 5.7 nm. A 210-mm  $f/4.8$  objective lens projects the image of a 25- $\mu\text{m}$  by 0.5-cm entrance slit on the water directly under the aircraft. The image of the slit is perpendicular to the flight line. At the nominal operating altitude of 600 m over the target, and a speed of 200 km/hr, the footprint of a ten-frame spectrum is approximately 18-m square.

The size of the footprint can be controlled by the operating altitude and speed of the aircraft, the focal length of the objective lens, and the number of frames per spectrum. This allows the spatial resolution to be varied to accommodate the needs of a particular survey. For example, in small bodies of water, turbidity patterns can be monitored. This flexibility is one reason the instrument is particularly adaptable to Corps of Engineers needs.

Flight lines were photographed with a 35-mm camera triggered every tenth dump to magnetic tape. The camera was aimed at the nadir. Using the

photographs, it was possible to precisely determine the flight line path relative to landmarks and buoys, and to locate the area covered for each spectrum to within 6 m.

Absolute instrument response is calibrated with a standard tungsten lamp traceable to the National Bureau of Standards. A krypton lamp and hydrogen Geissler tube are used for wavelength calibration.

The stored data on the magnetic tape were formatted to be read by an IBM 4341 at the NASA Goddard Institute for Space Studies (GISS) and were stored for further analysis. Codes were developed at GISS (Ungar, pers. comm.) to subtract dark current (baseline), and to incorporate the instrument response function and wavelength calibration for calculating the radiant power in  $\text{mW}/\text{cm}^2\text{-sr}$ . The results are plotted as a function of wavelength (Figure 2). For a detailed description of the instrument see Chiu and Collins (1978).

#### APPROACH

Because a portion of the reflected global radiance from water is from subsurface scattering, organic and inorganic material dispersed in the water would modify the spectrum of the reflected radiance (Richie *et al.*, 1976; Moore, 1980). Changes in turbidity due to run-off, dredging operations, or beginning algae blooms could be detected by changes in the spectral distribution of the reflected radiance (Richie *et al.*, 1976). Ideally, small concentrations of near-surface organic and inorganic suspended materials could be identified and quantified using the airborne spectroradiometer and computer-aided data

reduction. However, the needs of the Corps of Engineers do not require this level of sophistication, and although it would be useful, it is beyond the scope of this study. The present needs of the Corps are straightforward. Initially, ground truth data would be taken during an overflight and the signal calibrated. Subsequent flights would not require ground truth. Any difference of turbidity could be monitored and appropriate remedial action taken if required.

The study was divided between field and laboratory experiments. The purpose of the field experiments was to evaluate the operation and limitations of the airborne spectroradiometer and to obtain a better understanding of the problems of remote sensing of subsurface spectral radiance from water bodies. The laboratory experiments were run to obtain spectral data for known water quality conditions. Procedures were evaluated to separate the various components from the total reflected radiance and to correlate the spectral distribution of the subsurface reflectance with the organic/inorganic materials in the water.

## RESULTS

### FIELD EXPERIMENTS

The instrument was flown over various types of water bodies, and the reflected spectral signatures were recorded at the same time that *in situ* water quality measurements were taken. This was done to test and evaluate the instrument's response to various concentrations of suspended material in the water.

Flights were conducted over Lake Powell, Utah, and the coastal environments near Duck, North Carolina. The spectra were correlated with *in situ* ground truth water quality measurements. Flights were usually on the order of 16 km or less; therefore, different suspended sediment levels could be compared under conditions of fairly constant global illumination.

The Lake Powell spectra were taken on four separate flight lines (Figure 2). Three of the spectra were obtained within an hour of each other and the fourth, the Bullfrog Bay spectrum, was obtained a week earlier at approximately the same time of day (Merry, 1977). Secchi disk measurements for the Lake Powell spectra indicated that there was no bottom reflection (Table 1). Also, the flight line monitor photograph showed that the water surface was mirror-smooth with no specular sun image in the vertical direction. This is evidenced by low spectral response in the near-infrared region ( $>750$  nm). The contribution due to surface reflection of the sky can be ignored since it is almost totally limited to that portion of the sky within 0.86 degree of the zenith. Under these conditions the reflected radiance is almost completely from subsurface scattering.

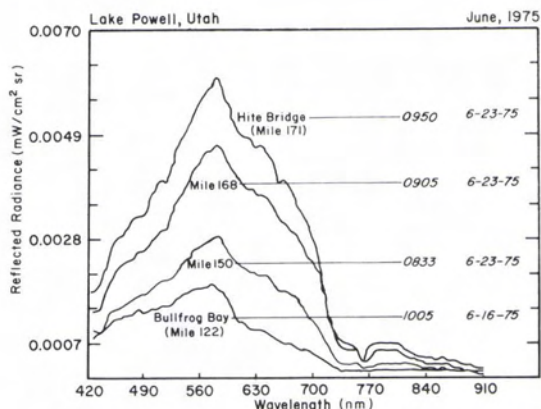


FIG. 2. Airborne spectroradiometer data from Lake Powell, Utah (after Merry, 1977).

The Lake Powell spectra (Figure 2) show increasing reflectance from Bullfrog Bay north toward Hite Bridge. There is a correlation between the increasing amplitude of the reflected radiance and the increasing sediment load from Bullfrog Bay to Hite Bridge (Table 1.). Considering the similarity of conditions during these runs, it is reasonable to conclude that this correlation is due to scattering from suspended sediments. At sediment loads of around 5 ppm, the level of detection is on the order of a few parts per million. The amplitude of the reflected radiance decreases nonlinearly with increasing turbidity, and the nonlinearity varies with wavelength. The very flat response in the long wavelength region ( $>750$  nm) of the Bullfrog Bay spectrum is due to the opacity of water in the near-infrared and the small amounts of suspended sediment.

At Duck, North Carolina, flight lines were flown about 5 km offshore, heading shoreward towards the Corps pier and continuing over Currituck Sound (Figure 3). Figure 4 shows the resulting spectra. The ocean spectrum was obtained about 1.5 km off the Corps Pier (maintained by the U.S. Army Coastal Engineering Research Center), and the sound spectrum was from the area around Buoy 4 (Figure 3). Table 2 shows the water quality information obtained at the time of the aircraft flight. The amount of dissolved solids in the two water environments differed and was only measured to indicate salinity conditions. Dissolved solids include colorless salts that are not amenable to passive remote sensing.

Because both the ocean and sound spectra were recorded on the same flight line, the global illumination was considered to be the same. However, the surface conditions were very different, as there were long waves in the ocean as compared to short, choppy waves in the sound. There were very few whitecaps on the ocean or sound during the flights.

A comparison of the Lake Powell Bullfrog Bay

TABLE 1. GROUND TRUTH WATER QUALITY DATA AT LAKE POWELL, UTAH (AFTER MERRY, 1977).

Location	Data	Secchi disk depth (m)	Suspended sediment concentration, filtered (mg/l)	Solar zenith angle (degrees)
Hite Bridge (Mile 171)	0950 hr	0.18	77.2	47.3
	23 June			
Mile 168	0905 hr	0.30	41.1	56.3
	23 June			
Mile 150	0833 hr	0.75	5.9	62.6
	23 June			
Bullfrog Bay (Mile 122)	1005 hr	4.50	4.9	44.4
	16 June			

spectra and the Duck ocean spectra illustrates the problem of sun glint. In both circumstances the water contained similar amounts of suspended sediment and organic material (chlorophyll). Tables 1 and 2 show the Duck ocean water to be as clear as the water in Bullfrog Bay; however, the Duck spectra show significant reflected radiance out to 900 nm. The amplitude of the oxygen absorption line shows substantial radiance at 760 nm. Because of the surface wave motion of the water, a portion of the sun glint is directed vertically upward to the radiometer. Spectral reflectance of the sun is a recognized problem in optical oceanography (Jerlov and Nielsen, 1974; Moore, 1980).

The differences between the Currituck Sound and ocean spectra (Figure 4) correspond to the ground truth shown in Table 2. The response in the 400- to 500-nm range is almost identical for the sound and ocean, and for this reason is believed to be specular reflection. This indicates that the amplitude of the specular reflectance over the entire range was the same for both spectra, even though the surface conditions were quite different. Therefore, the differences in these two spectra are principally due to differences in subsurface scattering of the various amounts of suspended sediment and the bottom reflection.

Currituck Sound is 0.5- to 2-m deep in the vicinity of Buoy 4. Large patches of grass occur on the bottom of the sound. The sound spectrum was dominated by the organic materials. The large response at 710 nm is typical of the reflected radiance from vegetation (Ungar *et al.*, 1977) and is in part due to reflection from subsurface vegetative growth.

This field work demonstrates that scattering from near-surface suspended sediment can be detected. At low sediment loads differences of 5 ppm of inorganic sediments can be measured. When scattering occurs from a mixture of organic and inorganic materials and bottom reflection, the reflected spectrum will have a distinctive distribution for a

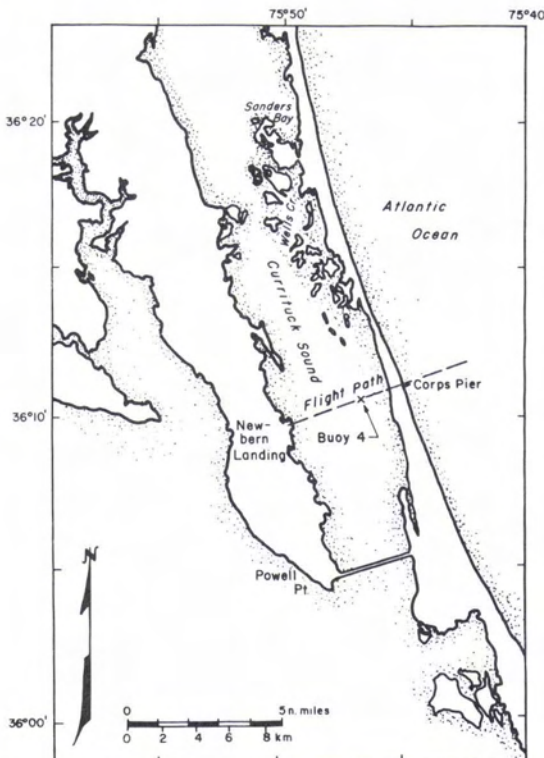


FIG. 3. Site location map of Duck, North Carolina, field experiments.

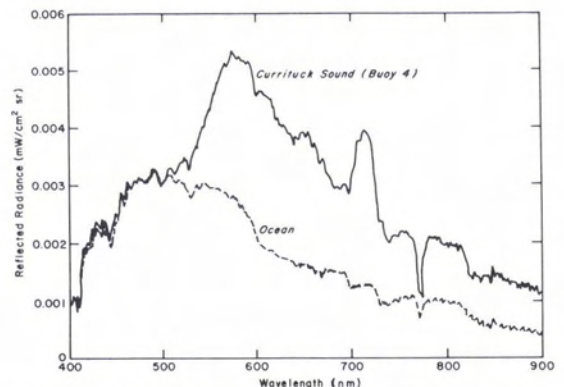


FIG. 4. Aircraft spectra from Duck, North Carolina.

TABLE 2. GROUND TRUTH WATER QUALITY DATA AT DUCK, NORTH CAROLINA.

Ocean, 1.5 km from pier (12 September 1978)					
Depth (m)		0.6	3.0	7.6	
Suspended solids (mg/l)		4.6	0.8	6.3	
Total dissolved solids (mg/l)		34,090	34,116	35,074	
Chlorophyll <i>a</i> (mg/m <sup>3</sup> )		2.7			
Currituck Sound, Buoy 4 (12 September 1978)					
Depth (m)	Surface	0.3	0.6	0.9	1.2
Suspended solids (mg/l)		16.2	12.4	15.0	32.0
Total dissolved solids (mg/l)		592	676	452	836
Chlorophyll <i>a</i> (mg/m <sup>3</sup> )	391.4				

particular mix of reflecting components and the spectrum of the global illumination. The modified spectral characteristics of a particular body of water caused by various types of suspended material can be empirically determined.

#### LABORATORY EXPERIMENTS

Preliminary field studies have shown that differences of 5 ppm of suspended particles can be detected by the airborne spectroradiometer (Merry, 1977). Due to variations in suspended sediment concentrations and surface conditions observed in field environments, an indoor tank 1-m square and 1-m deep was constructed to evaluate the instrument response under laboratory conditions. The tank depth could be varied by means of a movable bottom. The coating on the sides of the tank was optically black. The surface was illuminated by a high-intensity tungsten lamp. The lamp position was adjustable. A mechanical wave generator simulated a wind-roughened surface. The intention was not to exactly simulate an outdoor environment, but to maintain a controlled environment. The oxygen absorption line did not appear on the laboratory spectra because of the short path length of illumination.

*Surface conditions.* A serious problem in the interpretation of the spectral data is the separation of the surface specular reflection from the total reflected radiance. The ratio between relative intensity of the specular reflection and the total reflected radiance is a function of the conditions at the air/water interface. In calm waters, an unusual field condition, the specular reflection at nadir is at a minimum and the resulting spectra of reflected radiance are due primarily to subsurface scattering. This is because the sensor is looking at the nadir and the sun is not at the zenith; in calm water the image of the sun is not seen by the radiometer.

Under these conditions, the sky within 0.86 degree of the zenith is reflected into the sensor. An example of such conditions can be observed in the Lake Powell spectra (Figure 2). Usually in the field one encounters a wind-roughened surface, which will reflect an image of the sun into the sensor. The specular reflection is sometimes the highest intensity component of the reflected radiance.

The spectra of reflected radiance from smooth and wave-roughened water in the laboratory tank are shown in Figure 5. A sand and rock bottom was 90-cm below the surface. The illumination was provided by the tungsten lamp at a zenith angle of 20.6 degrees. The spectrum for the smooth surface is due to subsurface scattered light, mostly from the bottom. The rapid attenuation at wavelengths above 750 nm demonstrates the opaqueness of water in the near-infrared. The spectrum for the wave-roughened surface is the sum of specular reflection from the surface and subsurface reflection. The spectrum for the arithmetic difference is also shown (Figure 5).

The data recorded by the spectroradiometer are the sum of the specular reflection and subsurface scattering; therefore, if the spectral distribution and amplitude of the specular reflection are known, the spectrum of the subsurface scattering and primary illumination can be calculated. In addition, if the spectral distribution of the primary radiance and the Fresnel transmission coefficients are known, the subsurface illumination can then be determined. This would be extremely useful in the analysis of subsurface scattering spectra. A procedure for extracting the spectrum of the primary illumination from the spectrum of the total reflected radiance is described below.

*Polarization experiment.* The primary illumination of the water surface is the global radiance, which is the nonpolarized, parallel direct sunlight

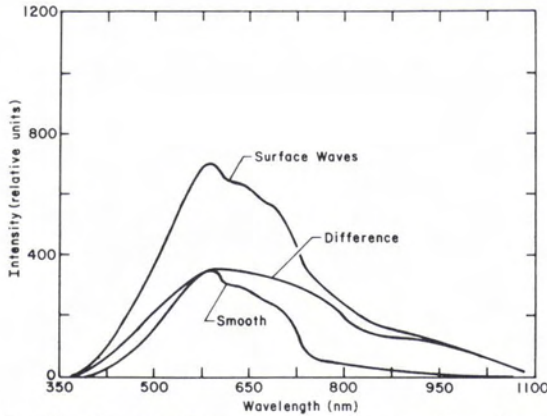


FIG. 5. Spectra of smooth water and a wind-roughened water surface.

and the partially polarized, nonparallel skylight. The plane of polarization of the skylight is a function of its direction. Both the direct sunlight and skylight are specularly reflected; however, the glint due to the direct sunlight is usually dominant. It is important to understand, however, that the skylight cannot be totally neglected, and its effect, especially in the shorter wavelengths, can be appreciable. The altitude of the sun is an important factor when comparing the influence of the skylight to the direct sunlight (Moon, 1940).

The Fresnel coefficients of reflection and transmission for light incident on a dielectric surface are a function of the angle of incidence and the orientation of the plane of polarization relative to the plane of incidence (Jackson, 1962). The ratio of the perpendicular and parallel (relative to the plane of incidence) components of the specular reflection is, therefore, a function of the angle of incidence. This fact plus the considerations of the previous paragraph can be used to separate the spectral distribution of the specular reflection of the direct sunlight from the spectrum of the total reflected radiance. This requires a rotatable polarizing filter, a depolarizing filter, accurate data of the solar zenith angle and solar azimuth, and direction of flight. The solar azimuth and flight direction data are used to locate the plane of incidence of the direct solar radiance. Because the sensor is pointed at the nadir and the direct solar radiance is a parallel beam, the angle of incidence for glint detected by the sensor will be one-half the solar zenith angle. Differences in intensities of the reflected radiance are recorded with the polarizing filter, parallel and perpendicular to the plane of incidence. From the data the amplitude and spectral distribution of the direct sunlight at the air/water interface can be determined.

The depolarizing filter is required because the instrument response function is dependent on the plane of polarization of the incoming light. This is due to the difference in efficiency of the diffraction

grating to light polarized parallel and perpendicular to the grating rulings. The instrument response function is measured with randomly polarized light.

This technique was tested in the laboratory and the results were encouraging (Figure 6). The target was a white reflector submerged in 27 cm of clear water with a wave-roughened surface illuminated by the tungsten lamp at a zenith angle of 31 degrees. Curves 1 and 2 are spectra of the parallel and perpendicular components to the plane of incidence of the total reflected radiance (Figure 6). Curve 3 is the arithmetic difference of curves 1 and 2 and is the spectral distribution of the specular reflection of the primary illumination. Curve 4, the subsurface scattering, is curve 3 normalized by means of the Fresnel coefficients and then subtracted from the calculated total reflected radiance. Curve 5 is the spectrum of a white reflector with calm water (no specular reflection) for comparison.

Curves 4 and 5 have a similarity. The important difference between them is that in the longer wavelengths the distribution shown in curve 4 did not go to zero as rapidly as that in curve 5. This means that the difference spectrum (curve 3) does not accurately represent the distribution of the specular reflection. The reasons for this are (1) the primary illumination source was not exactly parallel; and (2)

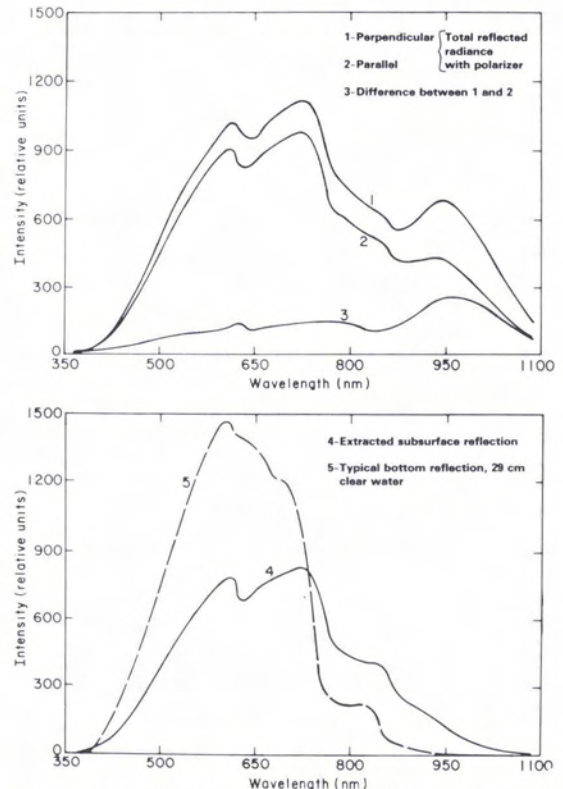


FIG. 6. Separation of specular reflection from total reflected radiance.

although the 210-mm objective lens of the spectrometer was focused at infinity, the finite dimensions of the entrance slit (25  $\mu\text{m}$  by 0.5 cm) and the closeness to the target (1 m) allowed specular reflection from planes that were not parallel to reach the sensor. The distortion in the shorter wavelengths (<650 nm) as compared to the clear water spectra was caused by the polarizer not being a neutral density filter.

**Instrument response to suspended materials.** To measure the instrument's response to suspended sediment concentrations, experiments with colloidal suspensions of montmorillonite clay and algae were run in the laboratory tank. The responses to both the clay and algae suspensions were measured individually and then in combination. The water depth was held at 90 cm. The only illumination was the high intensity tungsten lamp at a zenith angle of 20.6 degrees.

The results of the measurements with the montmorillonite clay suspensions are shown in Figure 7. The effective optical depth decreased as the concentration of suspended montmorillonite clay increased. This resulted in an increase in the amplitude of the reflected radiance. A comparison of the clear water spectrum to the 11.2-ppm spectrum in the vicinity of 650 nm and 800 nm shows a slight color difference between the suspended clay and sand bottom (Figure 7). The results indicate that differences on the order of 5 ppm of inorganic suspended sediment can be detected (Figure 7).

Various concentrations of blue-green algae compared to clear water over a white reflecting bottom (90-cm deep) are shown in Figure 8. The signal measured by the radiometer is the reflection from the sand bottom of the tank and is consequently attenuated by increasing concentrations of algae. The sensitivity to changes in varying concentrations of the algae is also less than for inorganic sediment. The concentration of the 500-ml curve is 440  $\text{mg}/\text{m}^3$  for all chlorophyll types (*a*, *b*, and *c*) (Figure 8).

Figure 9 shows the spectra of 4200 ml (916  $\text{mg}/\text{cm}^3$  of all chlorophyll types) of blue-green algae, clear water, and a combination of 4200 ml of blue-green algae and 218 ppm of montmorillonite clay. In the algae-clay spectrum the increased reflectance in the short and long wavelengths is expected; however, the further attenuation in the central wavelengths (550 nm to 680 nm) as compared to the algae spectrum is not presently understood. This could be due to an error of amplitude calculation in data reduction because of an incorrect recording of the *f*-stop of the objective lens of the radiometer. The amplitude of the spectrum of the clay-algae suspension should be on the order of intensity shown in the clay spectrum (Figure 7).

The spectral distribution of the algae-clay suspension is consistent with the results of the other tank experiments. In the near-infrared wavelengths (>750 nm) the response of clay is independent of

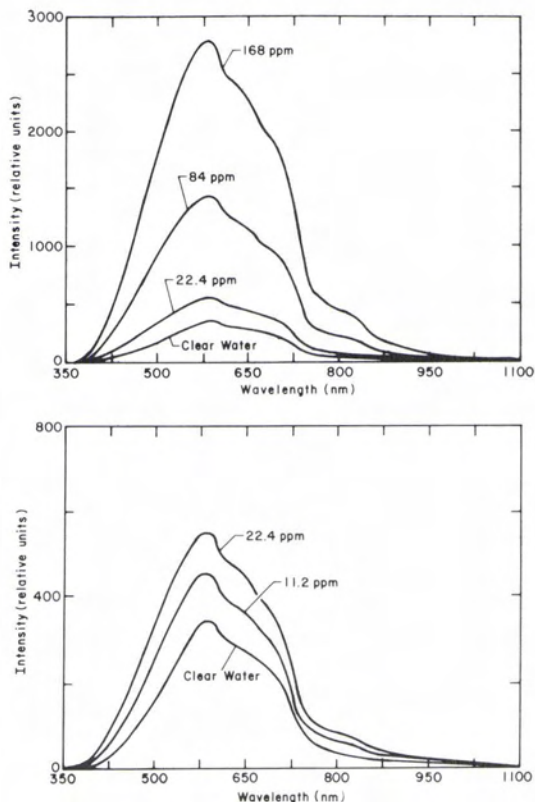


FIG. 7. Spectra of various concentrations of montmorillonite clay suspensions.

the presence of algae (Figure 9). In the visible wavelengths, where the light transmission path is longer than in the near-infrared, the amplitude of the increased reflectance due to the presence of suspended clay is attenuated because of the absorption by the algae. This illustrates how the ratios of the amplitudes of selected spectral bands become useful

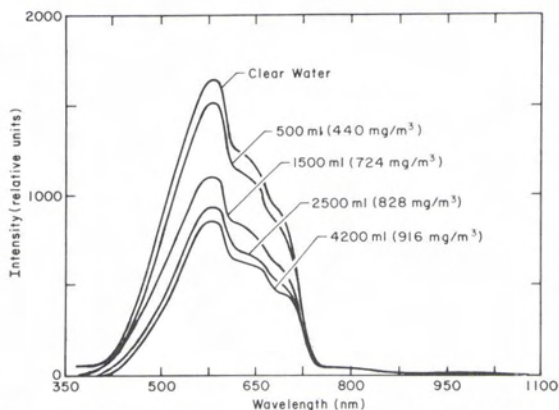


FIG. 8. Spectra of various amounts of algae. The algae is expressed in  $\text{mg}/\text{m}^3$  to include chlorophyll types *a*, *b*, and *c*.

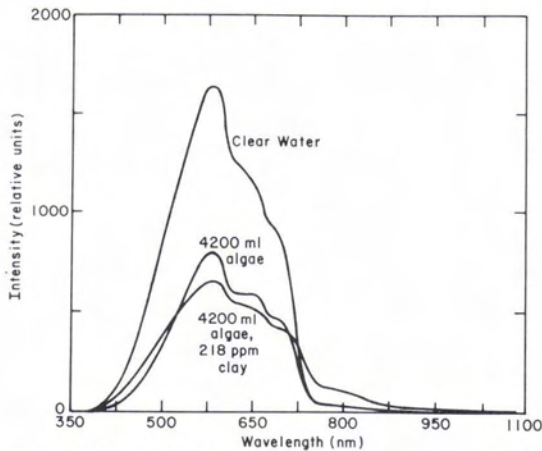


FIG. 9. Spectra of clear water, algae, and a mixture of clay and algae.

in determining the presence of suspended organic and inorganic materials.

#### SUMMARY AND CONCLUSIONS

A procedure for extracting the spectrum of direct sunlight from the spectrum of total reflected radiance has been described. Laboratory tests of this technique have been encouraging. The spectra of the reflectance from suspensions of organic and inorganic sediments, individually and in combination, were correlated with the amounts of the suspended materials in laboratory experiments. Differences of 5 ppm for inorganic suspensions can be detected. The response to organic suspensions is sensitive to the order of  $100 \text{ mg/m}^3$  in shallow water. The spectral distribution of the clay-algae suspension was consistent with the data of the individual clay and algae spectra; however, the amplitude of the clay-algae spectra was considerably less than would be expected.

Field work showed that suspended levels of inorganic materials can be resolved to 5 ppm. Suspended organic materials show a unique spectral signature; however, the accuracy is still to be determined.

The Chiu-Collins spectroradiometer system can provide adequate qualitative and quantitative information on suspended materials to be used in conjunction with ground truth for monitoring water quality changes in oceans, estuaries, lakes, and reservoirs. The footprint of the instrument is variable, which allows for changing the two-dimensional spa-

tial resolution. It may now be possible to define a water quality monitoring system using *in situ*, aircraft, and satellite data, which can supply users with various water quality parameters with a turnaround time of 24 hours.

#### ACKNOWLEDGMENTS

This study was sponsored under the Corps of Engineers Civil Works Remote Sensing Research Program, CWIS 31583, *Use of Aircraft Spectroradiometry to Determine Water Quality*. Appreciation is extended to Dr. Stephen G. Ungar and the NASA GISS programming staff for development of the computer algorithms for the airborne spectroradiometer system, and Dr. William Collins for the loan of the spectroradiometer and for technical assistance.

#### REFERENCES

- Chiu, H-Y, and W. Collins, 1978. A spectroradiometer for airborne remote sensing, *Photogrammetric Engineering and Remote Sensing*, vol. 44, no. 4, pp. 507-517.
- Hodgson, R. M., F. M. Cady, and D. Pairman, 1981. A solid-state airborne sensing system for remote sensing, *Photogrammetric Engineering and Remote Sensing*, vol. 47, no. 2, pp. 177-182.
- Jackson, J. D., 1962. *Classical electrodynamics*, John Wiley and Sons, Inc.: New York, New York.
- Jerlov, N. G., and E. S. Nielsen, 1974. *Optical aspects of oceanography*, Academic Press: London, England.
- Merry, C. J., 1977. *Airborne spectroradiometer data compared with ground water-turbidity measurements at Lake Powell, Utah, Correlation and quantification of data*, CRREL Special Report 77-28 (master's thesis, Dartmouth College), 43 p.
- Moon, P., 1940. Proposed standard solar-radiance curves for engineering use, *Journal of the Franklin Institute*, vol. 230, no. 5, pp. 583-618.
- Moore, G. K., 1980. Satellite remote sensing of water turbidity, *Hydrological Sciences-Bulletin*, vol. 25, no. 4, pp. 407-421.
- Ritchie, J. C., F. R. Schiebe, and J. R. McHenry, 1976. Remote sensing of suspended sediments in surface waters, *Photogrammetric Engineering and Remote Sensing*, vol. 42, no. 12, pp. 1539-1545.
- Ungar, S. G., W. Collins, J. C. Coiner, D. Egbert, R. Kiang, T. Cary, P. Coulter, N. Landau, E. Matthews, S. Lytle, K. Prentice, N. Lytle, A. Rodriguez, J. Flamholz, W. Beck, N. Wasserman, D. Angier, and S. Lydiard, 1977. *Atlas of selected crop spectra, Imperial Valley, California*, NASA Institute for Space Studies/Goddard Space Flight Center: New York, New York.

(Received 28 June 1982; revised and accepted 25 November 1983)